ARMY RESEARCH LABORATORY

Addendum to ARL-TR-4005
Adding Weather to Wargames

by Sean G. O'Brien and Richard C. Shirkey

ARL-TR-4460 **May 2008**

NOTICES

Disclaimers

The findings in this report are not to be construed as an official Department of the Army position unless so designated by other authorized documents.

Citation of manufacturer's or trade names does not constitute an official endorsement or approval of the use thereof.

Destroy this report when it is no longer needed. Do not return it to the originator.

Army Research Laboratory
White Sands Missile Range, NM 88008-5501

ARL-TR-4460 **May 2008**

Addendum to ARL-TR-4005
Adding Weather to Wargames

Sean G. O'Brien and Richard C. Shirkey
Computational Information Sciences Directorate, ARL

REPORT DOCUMENTATION PAGE

Form Approved
OMB No. 0704-0188

1. REPORT DATE *(DD-MM-YYYY)*	2. REPORT TYPE	3. DATES COVERED (From - To)
May 2008	Final	2003-2006

4. TITLE AND SUBTITLE
Addendum to ARL-TR-4005 Adding Weather to Wargames

5a. CONTRACT NUMBER

5b. GRANT NUMBER

5c. PROGRAM ELEMENT NUMBER

6. AUTHOR(S)
Sean G. O'Brien and Richard C. Shirkey

5d. PROJECT NUMBER

5e. TASK NUMBER

5f. WORK UNIT NUMBER

7. PERFORMING ORGANIZATION NAME(S) AND ADDRESS(ES)
U.S. Army Research Laboratory
Computational and Information Sciences Directorate
Battlefield Environment Division (ATTN: AMSRD-ARL-CI-EE)
White Sands Missile Range, NM 88002-5501

8. PERFORMING ORGANIZATION REPORT NUMBER
ARL-TR-4460

9. SPONSORING/MONITORING AGENCY NAME(S) AND ADDRESS(ES)

10. SPONSOR/MONITOR'S ACRONYM(S)

11. SPONSOR/MONITOR'S REPORT NUMBER(S)

12. DISTRIBUTION/AVAILABILITY STATEMENT
Approved for public release; distribution is unlimited.

13. SUPPLEMENTARY NOTES

14. ABSTRACT
This addendum presents updated graphical representations of the selected Target Acquisition Weapons Software (TAWS) output and also the coefficients for the third order polynomial fits that originally appeared in appendices B and C.

15. SUBJECT TERMS
Wargames, weather, sensors, rules, parametric curve fits, target acquisition

16. SECURITY CLASSIFICATION OF:			17. LIMITATION OF ABSTRACT	18. NUMBER OF PAGES	19a. NAME OF RESPONSIBLE PERSON
a. REPORT	b. ABSTRACT	c. THIS PAGE			Richard C. Shirkey
U	U	U	UU	44	19b. TELEPHONE NUMBER (*Include area code*) (575) 678-1570

Standard Form 298 (Rev. 8/98)
Prescribed by ANSI Std. Z39.1

Contents

List of Figures

List of Tables

Summary

The method used for calculation of the third order polynomials in the original report "Adding Weather to Wargames" (*1*), did not provide a satisfactory fit in all cases. In addition, we ascertained that some spurious data from the Target Acquisition Weapons Software (TAWS) output were used in the calculation of the parametric curves. Therefore, we have redone the graphs and recalculated the polynomial coefficients for the parametric curves that appeared in appendices B and C using a different technique (*2*). To assure a better fit, we added 3 "synthetic" data points between the 4 normalized detection ranges at visibilities of 0.1, 1.0, 10.0, and 100.0. We assumed that the 4 input data points are evenly spaced in ln space, so that the 3 synthetic points are midway in both ln x and ln y. The polynomial now takes the following form:

$$Ndr = a_0 + a_1 * \ln(V) + a_2 * \ln(V)^2 + a_3 * \ln(V)^3, \quad (1)$$

Where Ndr is the normalized detection range, V is the visibility in km, and a_0-a_3 are the third order polynomial coefficients.

Appendices B and C have been updated with corrected versions of the graphs for normalized detection range vs. visibility, and with the new third order polynomial coefficients.

History

Employing the capability of the Target Acquisition Weapons Software (TAWS) tactical decision aid, and the rules embodied in the Integrated Weather Effects Decision Aid (IWEDA) we developed techniques that allowed significant improvement in weather effects and impacts for wargames. TAWS was run for numerous and varied weather conditions; the resultant database was subsequently used to construct third-order polynomial curves to represent infrared sensors acquiring targets under those weather conditions. IWEDA rules were used in determination of go/no-go weather situations for platforms or systems. We found that the wargame realism was increased without impacting the run time. While these techniques are applicable to wargames in general, we tested them by incorporation into the Advanced Warfighting Simulation (AWARS) model. AWARS was modified to incorporate weather impacts upon sensor operation and platform mobility. These modifications included revision of the direct-fire sensor detection algorithm to reflect variations of the maximum number of resolution cycles over the direct fire target with meteorological visibility, time of day, sky cover, target state, and haze aerosol type. The speed of these computations was an important consideration, so the parametric fit technique was selected after a favorable comparison with table look-up methods. Weather effects upon combatant platform mobility were modeled by implementation of IWEDA rules classes for both helicopters and fixed-wing aircraft platforms. The impacts of these modifications in both the presence and absence of adverse weather conditions were tested and are summarized.

2. Addendum to Appendices B and C

A special note about Monikers used in appendices B and C.

Table A-4 applies to both appendices B and C.

Each moniker, used in the following table, is a concatenation of the various atmospheric conditions that we used; with the exception of the 0900 time period, the first three characters of each atmospheric condition were used. This cipher is presented in table A-4.

Table A-4. Monikers and their meaning as used in the various tables and figures in appendices B and C.

Moniker	Meaning
Fog	Fog
Rur	Rural
Tan	Tank
Exe	Exercised
Off	Inactive
900	0900
150	1500
Win	Winter

Table A-4. Monikers and their meaning as used in the various tables and figures in appendices B and C (continued).

Moniker	**Meaning**
Sum	Summer
Nor	North
Sou	South
Eas	East
Wes	West
Ove	Overcast
Cle	Clear

Appendix B. Third-Order Polynomial Coefficients and their Curves for the Fog Aerosol for a Narrow Field of View (NFOV) and Wide Field of View (WFOV) Average Infrared (IR) Sensor

Table B-1. Third-order polynomial coefficients curve fit to averaged quantities as represented by moniker for average sensor viewing through a fog aerosol. WFOV results are shown.

Moniker	a0	a1	a2	a3	Average Maximum Detection Range
150CleFog	0.7182	0.1504	-0.0111	-0.0018	3.59
150OveFog	0.7051	0.1536	-0.0098	-0.0021	3.59
900CleFog	0.6241	0.1648	-0.0022	-0.0034	3.42
900OveFog	0.5536	0.1661	0.0036	-0.0041	3.25
Tan900CleFog	0.7090	0.1455	-0.0100	-0.0017	2.69
Tan150CleFog	0.8033	0.1232	-0.0185	0.0002	2.80
Tan900OveFog	0.6682	0.1527	-0.0063	-0.0024	2.68
Tan150OveFog	0.7953	0.1260	-0.0180	0.0001	2.79
TanExe150OveFog	0.8185	0.1193	-0.0205	0.0007	2.82
TanExe900OveFog	0.7568	0.1391	-0.0147	-0.0009	2.78
TanExe150CleFog	0.8193	0.1183	-0.0201	0.0006	2.82
TanExe900CleFog	0.7667	0.1352	-0.0152	-0.0007	2.78
TanOff900CleFog	0.6369	0.1580	-0.0036	-0.0029	2.58
TanOff150CleFog	0.7872	0.1281	-0.0170	-0.0002	2.78
TanOff150OveFog	0.7722	0.1327	-0.0155	-0.0006	2.76
TanOff900OveFog	0.5662	0.1674	0.0032	-0.0041	2.56
TanOff900SumOveFog	0.5723	0.1665	0.0023	-0.0040	2.45
TanOff900WinOveFog	0.5351	0.1712	0.0062	-0.0047	2.63
TanOff150SumOveFog	0.7868	0.1275	-0.0167	-0.0002	2.77
TanOff150WinOveFog	0.7284	0.1484	-0.0124	-0.0015	2.74
TanOff900NorOveFog	0.5555	0.1648	0.0034	-0.0040	2.51
TanOff900EasOveFog	0.5345	0.1637	0.0061	-0.0043	2.44
TanOff900WesOveFog	0.6175	0.1712	-0.0007	-0.0040	2.66
TanOff900SouOveFog	0.5486	0.1688	0.0043	-0.0043	2.60
TanExe900SumOveFog	0.7575	0.1385	-0.0146	-0.0009	2.78
TanExe900WinOveFog	0.7517	0.1415	-0.0144	-0.0010	2.79
TanExe150SumOveFog	0.8231	0.1169	-0.0207	0.0008	2.81
TanExe150WinOveFog	0.8012	0.1265	-0.0193	0.0003	2.81
TanExe900NorOveFog	0.8309	0.1168	-0.0220	0.0010	2.85
TanExe900EasOveFog	0.7412	0.1441	-0.0134	-0.0012	2.76
TanExe900WesOveFog	0.7599	0.1393	-0.0159	-0.0007	2.80
TanExe900SouOveFog	0.6952	0.1557	-0.0077	-0.0026	2.72
TanExe150NorOveFog	0.8464	0.1112	-0.0232	0.0014	2.85
TanExe150EasOveFog	0.8219	0.1179	-0.0208	0.0008	2.81
TanExe150WesOveFog	0.8185	0.1193	-0.0207	0.0007	2.83
TanExe150SouOveFog	0.7870	0.1287	-0.0173	-0.0001	2.78

Table B-1. Third-order polynomial coefficients curve fit to averaged quantities as represented by moniker for average sensor viewing through a fog aerosol. WFOV results are shown (continued).

Moniker	a0	a1	a2	a3	Average Maximum Detection Range
TanExe900NorCleFog	0.8335	0.1162	-0.0223	0.0011	2.85
TanExe900EasCleFog	0.7429	0.1444	-0.0140	-0.0011	2.76
TanExe900WesCleFog	0.8014	0.1232	-0.0179	0.0001	2.81
TanExe900SouCleFog	0.6892	0.1565	-0.0067	-0.0027	2.72
TanExe150NorCleFog	0.8514	0.1092	-0.0234	0.0015	2.85
TanExe150EasCleFog	0.8345	0.1130	-0.0214	0.0010	2.83
TanExe150WesCleFog	0.8071	0.1221	-0.0189	0.0003	2.80
TanExe150SouCleFog	0.7842	0.1287	-0.0166	-0.0003	2.79
TanOff900NorCleFog	0.6124	0.1661	-0.0014	-0.0035	2.49
TanOff900EasCleFog	0.5519	0.1665	0.0043	-0.0042	2.40
TanOff900WesCleFog	0.7673	0.1361	-0.0163	-0.0005	2.77
TanOff900SouCleFog	0.5699	0.1695	0.0030	-0.0042	2.59
TanOff150NorCleFog	0.7812	0.1296	-0.0161	-0.0004	2.77
TanOff150EasCleFog	0.8207	0.1188	-0.0211	0.0008	2.80
TanOff150WesCleFog	0.7811	0.1300	-0.0164	-0.0003	2.77
TanOff150SouCleFog	0.7657	0.1339	-0.0144	-0.0008	2.76
TanOff900SumNorCleFog	0.5304	0.1487	0.0030	-0.0029	2.07
TanOff900SumEasCleFog	0.5475	0.1590	0.0016	-0.0032	2.58
TanOff900SumWesCleFog	0.7699	0.1366	-0.0174	-0.0003	2.78
TanOff900SumSouCleFog	0.5875	0.1760	0.0021	-0.0045	2.70
TanOff150SumNorCleFog	0.7726	0.1317	-0.0150	-0.0006	2.75
TanOff150SumEasCleFog	0.8275	0.1168	-0.0220	0.0010	2.80
TanOff150SumWesCleFog	0.7937	0.1252	-0.0173	0.0000	2.78
TanOff150SumSouCleFog	0.7975	0.1246	-0.0179	0.0001	2.78
TanOff900WinNorCleFog	0.6554	0.1679	-0.0042	-0.0035	2.72
TanOff90Win0EasCleFog	0.6038	0.1802	0.0008	-0.0046	2.69
TanOff900WinWesCleFog	0.7554	0.1429	-0.0166	-0.0006	2.77
TanOff900WinSouCleFog	0.5575	0.1651	0.0033	-0.0040	2.78
TanOff150WinNorCleFog	0.7845	0.1301	-0.0171	-0.0002	2.81
TanOff150WinEasCleFog	0.8006	0.1248	-0.0183	0.0001	2.79
TanOff150WinWesCleFog	0.7419	0.1449	-0.0138	-0.0012	2.75
TanOff150WinSouCleFog	0.6910	0.1564	-0.0070	-0.0027	2.74
TanExe900SumNorCleFog	0.8276	0.1173	-0.0214	0.0009	2.85
TanExe900SumEasCleFog	0.7327	0.1466	-0.0125	-0.0015	2.75
TanExe900SumWesCleFog	0.8008	0.1229	-0.0176	0.0001	2.81
TanExe900SumSouCleFog	0.7083	0.1520	-0.0091	-0.0022	2.74
TanExe150SumNorCleFog	0.8498	0.1091	-0.0234	0.0015	2.85
TanExe150SumEasCleFog	0.8344	0.1121	-0.0209	0.0009	2.82
TanExe150SumWesCleFog	0.8090	0.1212	-0.0191	0.0004	2.80
TanExe150SumSouCleFog	0.8009	0.1223	-0.0177	0.0001	2.80
TanExe900WinNorCleFog	0.8514	0.1138	-0.0250	0.0016	2.85
TanExe90Win0EasCleFog	0.7675	0.1396	-0.0177	-0.0004	2.78
TanExe900WinWesCleFog	0.8006	0.1249	-0.0183	0.0001	2.82

Table B-1. Third-order polynomial coefficients curve fit to averaged quantities as represented by moniker for average sensor viewing through a fog aerosol. WFOV results are shown (continued).

Moniker	a0	a1	a2	a3	Average Maximum Detection Range
TanExe900WinSouCleFog	0.6819	0.1585	-0.0060	-0.0029	2.75
TanExe150WinNorCleFog	0.8608	0.1096	-0.0251	0.0017	2.85
TanExe150WinEasCleFog	0.8311	0.1164	-0.0221	0.0010	2.85
TanExe150WinWesCleFog	0.8003	0.1249	-0.0183	0.0001	2.81
TanExe150WinSouCleFog	0.7350	0.1463	-0.0130	-0.0014	2.76
TanOff900SumNorOveFog	0.5525	0.1583	0.0030	-0.0035	2.01
TanOff900SumEasOveFog	0.5162	0.1608	0.0080	-0.0044	2.28
TanOff900SumWesOveFog	0.6465	0.1725	-0.0044	-0.0036	2.67
TanOff900SumSouOveFog	0.5421	0.1674	0.0051	-0.0043	2.53
TanOff150SumNorOveFog	0.7724	0.1328	-0.0156	-0.0005	2.74
TanOff150SumEasOveFog	0.8011	0.1230	-0.0180	0.0001	2.78
TanOff150SumWesOveFog	0.8003	0.1237	-0.0182	0.0002	2.78
TanOff150SumSouOveFog	0.7734	0.1307	-0.0148	-0.0006	2.76
TanOff900WinNorOveFog	0.5529	0.1669	0.0035	-0.0040	2.69
TanOff900Win0EasOveFo	0.5323	0.1726	0.0073	-0.0049	2.53
TanOff900WinWesOveFog	0.5287	0.1738	0.0080	-0.0051	2.62
TanOff900WinSouOveFog	0.5308	0.1692	0.0045	-0.0042	2.74
TanOff150WinNorOveFog	0.7340	0.1479	-0.0137	-0.0013	2.74
TanOff150WinEasOveFog	0.7421	0.1448	-0.0139	-0.0012	2.74
TanOff150WinWesOveFog	0.7381	0.1459	-0.0134	-0.0013	2.74
TanOff150WinSouOveFog	0.6992	0.1547	-0.0085	-0.0024	2.73
TanExe900SumNorOveFog	0.8276	0.1173	-0.0214	0.0009	2.85
TanExe900SumEasOveFog	0.7380	0.1453	-0.0135	-0.0012	2.77
TanExe900SumWesOveFog	0.7713	0.1347	-0.0165	-0.0004	2.78
TanExe900SumSouOveFog	0.6931	0.1563	-0.0073	-0.0027	2.71
TanExe150SumNorOveFog	0.8420	0.1112	-0.0224	0.0012	2.85
TanExe150SumEasOveFog	0.8283	0.1157	-0.0215	0.0010	2.81
TanExe150SumWesOveFog	0.8244	0.1167	-0.0210	0.0009	2.81
TanExe150SumSouOveFog	0.7978	0.1241	-0.0178	0.0001	2.78
TanExe900WinNorOveFog	0.8411	0.1163	-0.0235	0.0012	2.85
TanExe900WinEasOveFog	0.7405	0.1454	-0.0138	-0.0012	2.78
TanExe900WinWesOveFog	0.7405	0.1454	-0.0138	-0.0012	2.78
TanExe900WinSouOveFog	0.6846	0.1585	-0.0064	-0.0029	2.75
TanExe150WinNorOveFog	0.8516	0.1133	-0.0247	0.0015	2.85
TanExe150WinEasOveFog	0.8029	0.1242	-0.0188	0.0002	2.81
TanExe150WinWesOveFog	0.8003	0.1249	-0.0183	0.0001	2.81
TanExe150WinSouOveFog	0.7500	0.1433	-0.0153	-0.0009	2.77

Table B-2. Third-order polynomial coefficients curve fit to averaged quantities as represented by moniker for average sensor viewing through a fog aerosol. NFOV results are shown. Coefficients in blue have associated curves presented in the graphs in this appendix.

Moniker	a0	a1	a2	a3	Average Maximum Detection Range
150CleFog	0.3553	0.2145	0.0247	-0.0089	8.88
150OveFog	0.3459	0.2124	0.0252	-0.0088	8.88
900CleFog	0.3014	0.1968	0.0262	-0.0078	8.52
900OveFog	0.2704	0.1762	0.0251	-0.0063	8.22
Tan900CleFog	0.3469	0.2067	0.0237	-0.0082	7.59
Tan150CleFog	0.4111	0.2204	0.0205	-0.0088	7.80
Tan900OveFog	0.3241	0.1972	0.0240	-0.0076	7.62
Tan150OveFog	0.4026	0.2206	0.0214	-0.0089	7.80
TanExe150OveFog	0.4226	0.2205	0.0192	-0.0087	7.80
TanExe900OveFog	0.3759	0.2189	0.0232	-0.0089	7.80
TanExe150CleFog	0.4285	0.2201	0.0187	-0.0086	7.80
TanExe900CleFog	0.3835	0.2185	0.0224	-0.0088	7.80
TanOff900CleFog	0.3008	0.1909	0.0251	-0.0073	7.32
TanOff150CleFog	0.3936	0.2203	0.0223	-0.0090	7.80
TanOff150OveFog	0.3824	0.2202	0.0234	-0.0091	7.80
TanOff900OveFog	0.2612	0.1697	0.0249	-0.0058	7.39
TanOff900SumOveFog	0.2613	0.1694	0.0248	-0.0058	7.20
TanOff900WinOveFog	0.2451	0.1715	0.0267	-0.0061	8.02
TanOff150SumOveFog	0.3904	0.2187	0.0226	-0.0090	7.80
TanOff150WinOveFog	0.3536	0.2228	0.0261	-0.0095	7.80
TanOff900NorOveFog	0.2510	0.1652	0.0247	-0.0055	7.30
TanOff900EasOveFog	0.2568	0.1647	0.0244	-0.0054	7.02
TanOff900WesOveFog	0.2774	0.1803	0.0255	-0.0066	7.80
TanOff900SouOveFog	0.2546	0.1658	0.0247	-0.0055	7.36
TanExe900SumOveFog	0.3758	0.2195	0.0234	-0.0090	7.80
TanExe900WinOveFog	0.3827	0.2236	0.0230	-0.0092	7.80
TanExe150SumOveFog	0.4251	0.2197	0.0191	-0.0086	7.80
TanExe150WinOveFog	0.4138	0.2226	0.0198	-0.0088	7.80
TanExe900NorOveFog	0.4352	0.2208	0.0176	-0.0084	7.80
TanExe900EasOveFog	0.3677	0.2209	0.0243	-0.0092	7.80
TanExe900WesOveFog	0.3761	0.2218	0.0238	-0.0092	7.80
TanExe900SouOveFog	0.3237	0.2086	0.0264	-0.0086	7.80
TanExe150NorOveFog	0.4503	0.2187	0.0162	-0.0082	7.80
TanExe150EasOveFog	0.4280	0.2209	0.0186	-0.0086	7.80
TanExe150WesOveFog	0.4203	0.2207	0.0196	-0.0087	7.80
TanExe150SouOveFog	0.3916	0.2209	0.0224	-0.0090	7.80
TanExe900NorCleFog	0.4362	0.2207	0.0174	-0.0084	7.80
TanExe900EasCleFog	0.3601	0.2195	0.0248	-0.0092	7.80
TanExe900WesCleFog	0.4152	0.2220	0.0200	-0.0088	7.80
TanExe900SouCleFog	0.3213	0.2073	0.0266	-0.0086	7.80
TanExe150NorCleFog	0.4537	0.2182	0.0159	-0.0081	7.80
TanExe150EasCleFog	0.4446	0.2189	0.0171	-0.0083	7.80

Table B-2. Third-order polynomial coefficients curve fit to averaged quantities as represented by moniker for average sensor viewing through a fog aerosol. NFOV results are shown. Coefficients in blue have associated curves presented in the graphs in this appendix (continued).

Moniker	a0	a1	a2	a3	Average Maximum Detection Range
TanExe150WesCleFog	0.4190	0.2209	0.0197	-0.0087	7.80
TanExe150SouCleFog	0.3963	0.2214	0.0221	-0.0090	7.80
TanOff900NorCleFog	0.2752	0.1826	0.0257	-0.0067	7.10
TanOff900EasCleFog	0.2638	0.1730	0.0254	-0.0061	6.79
TanOff900WesCleFog	0.3784	0.2220	0.0240	-0.0093	7.80
TanOff900SouCleFog	0.2566	0.1715	0.0253	-0.0059	7.36
TanOff150NorCleFog	0.3854	0.2191	0.0231	-0.0090	7.80
TanOff150EasCleFog	0.4215	0.2208	0.0195	-0.0087	7.80
TanOff150WesCleFog	0.3898	0.2205	0.0225	-0.0090	7.80
TanOff150SouCleFog	0.3775	0.2203	0.0238	-0.0092	7.80
TanOff900SumNorCleFog	0.2300	0.1521	0.0238	-0.0044	6.23
TanOff900SumEasCleFog	0.2621	0.1658	0.0228	-0.0052	7.39
TanOff900SumWesCleFog	0.3780	0.2226	0.0242	-0.0094	7.80
TanOff900SumSouCleFog	0.2586	0.1748	0.0257	-0.0062	7.70
TanOff150SumNorCleFog	0.3752	0.2169	0.0240	-0.0090	7.80
TanOff150SumEasCleFog	0.4249	0.2201	0.0193	-0.0087	7.80
TanOff150SumWesCleFog	0.3964	0.2191	0.0219	-0.0089	7.80
TanOff150SumSouCleFog	0.3976	0.2194	0.0218	-0.0089	7.80
TanOff900WinNorCleFog	0.3070	0.2138	0.0291	-0.0093	7.80
TanOff90Win0EasCleFog	0.2742	0.1938	0.0283	-0.0078	7.80
TanOff900WinWesCleFog	0.3738	0.2238	0.0239	-0.0093	7.80
TanOff900WinSouCleFog	0.2534	0.1781	0.0264	-0.0064	8.43
TanOff150WinNorCleFog	0.3937	0.2226	0.0226	-0.0092	7.80
TanOff150WinEasCleFog	0.4114	0.2225	0.0202	-0.0089	7.80
TanOff150WinWesCleFog	0.3676	0.2234	0.0248	-0.0094	7.80
TanOff150WinSouCleFog	0.3277	0.2200	0.0281	-0.0096	7.80
TanExe900SumNorCleFog	0.4310	0.2214	0.0179	-0.0085	7.80
TanExe900SumEasCleFog	0.3519	0.2202	0.0255	-0.0093	7.80
TanExe900SumWesCleFog	0.4141	0.2220	0.0202	-0.0088	7.80
TanExe900SumSouCleFog	0.3349	0.2170	0.0272	-0.0093	7.80
TanExe150SumNorCleFog	0.4477	0.2186	0.0168	-0.0083	7.80
TanExe150SumEasCleFog	0.4443	0.2186	0.0174	-0.0084	7.80
TanExe150SumWesCleFog	0.4203	0.2203	0.0197	-0.0087	7.80
TanExe150SumSouCleFog	0.4091	0.2205	0.0208	-0.0089	7.80
TanExe900WinNorCleFog	0.4553	0.2194	0.0148	-0.0080	7.80
TanExe90Win0EasCleFog	0.3801	0.2240	0.0231	-0.0092	7.80
TanExe900WinWesCleFog	0.4160	0.2225	0.0196	-0.0088	7.80
TanExe900WinSouCleFog	0.3257	0.2201	0.0284	-0.0096	7.80
TanExe150WinNorCleFog	0.4675	0.2174	0.0137	-0.0078	7.80
TanExe150WinEasCleFog	0.4410	0.2201	0.0170	-0.0083	7.80
TanExe150WinWesCleFog	0.4133	0.2225	0.0200	-0.0088	7.80
TanExe150WinSouCleFog	0.3655	0.2233	0.0250	-0.0094	7.80
TanOff900SumNorOveFog	0.2422	0.1588	0.0238	-0.0049	6.02

Table B-2. Third-order polynomial coefficients curve fit to averaged quantities as represented by moniker for average sensor viewing through a fog aerosol. NFOV results are shown. Coefficients in blue have associated curves presented in the graphs in this appendix (continued).

Moniker	a0	a1	a2	a3	Average Maximum Detection Range
TanOff900SumEasOveFog	0.2482	0.1568	0.0232	-0.0047	7.21
TanOff900SumWesOveFog	0.2877	0.1875	0.0261	-0.0072	7.80
TanOff900SumSouOveFog	0.2503	0.1628	0.0248	-0.0053	7.19
TanOff150SumNorOveFog	0.3751	0.2166	0.0240	-0.0090	7.80
TanOff150SumEasOveFog	0.4091	0.2205	0.0208	-0.0089	7.80
TanOff150SumWesOveFog	0.3986	0.2199	0.0217	-0.0089	7.80
TanOff150SumSouOveFog	0.3786	0.2175	0.0237	-0.0090	7.80
TanOff900WinNorOveFog	0.2425	0.1710	0.0269	-0.0061	8.58
TanOff900Win0EasOveFo	0.2395	0.1671	0.0266	-0.0058	7.66
TanOff900WinWesOveFog	0.2470	0.1738	0.0267	-0.0062	7.79
TanOff900WinSouOveFog	0.2541	0.1755	0.0264	-0.0063	8.43
TanOff150WinNorOveFog	0.3530	0.2228	0.0262	-0.0096	7.80
TanOff150WinEasOveFog	0.3670	0.2234	0.0248	-0.0094	7.80
TanOff150WinWesOveFog	0.3619	0.2231	0.0255	-0.0095	7.80
TanOff150WinSouOveFog	0.3324	0.2211	0.0278	-0.0096	7.80
TanExe900SumNorOveFog	0.4335	0.2207	0.0179	-0.0085	7.80
TanExe900SumEasOveFog	0.3658	0.2219	0.0247	-0.0093	7.80
TanExe900SumWesOveFog	0.3799	0.2227	0.0239	-0.0093	7.80
TanExe900SumSouOveFog	0.3230	0.2090	0.0265	-0.0086	7.80
TanExe150SumNorOveFog	0.4461	0.2188	0.0169	-0.0083	7.80
TanExe150SumEasOveFog	0.4326	0.2201	0.0182	-0.0085	7.80
TanExe150SumWesOveFog	0.4230	0.2199	0.0195	-0.0087	7.80
TanExe150SumSouOveFog	0.3985	0.2194	0.0216	-0.0089	7.80
TanExe900WinNorOveFog	0.4499	0.2200	0.0154	-0.0081	7.80
TanExe900WinEasOveFog	0.3771	0.2239	0.0235	-0.0093	7.80
TanExe900WinWesOveFog	0.3752	0.2238	0.0238	-0.0093	7.80
TanExe900WinSouOveFog	0.3266	0.2202	0.0283	-0.0096	7.80
TanExe150WinNorOveFog	0.4595	0.2192	0.0142	-0.0079	7.80
TanExe150WinEasOveFog	0.4160	0.2225	0.0196	-0.0088	7.80
TanExe150WinWesOveFog	0.4123	0.2225	0.0201	-0.0088	7.80
TanExe150WinSouOveFog	0.3666	0.2234	0.0249	-0.0094	7.80

The coefficients displayed in blue in table B-2 have associated curves that are presented in the following graphs labeled figures B-1 through B-15.

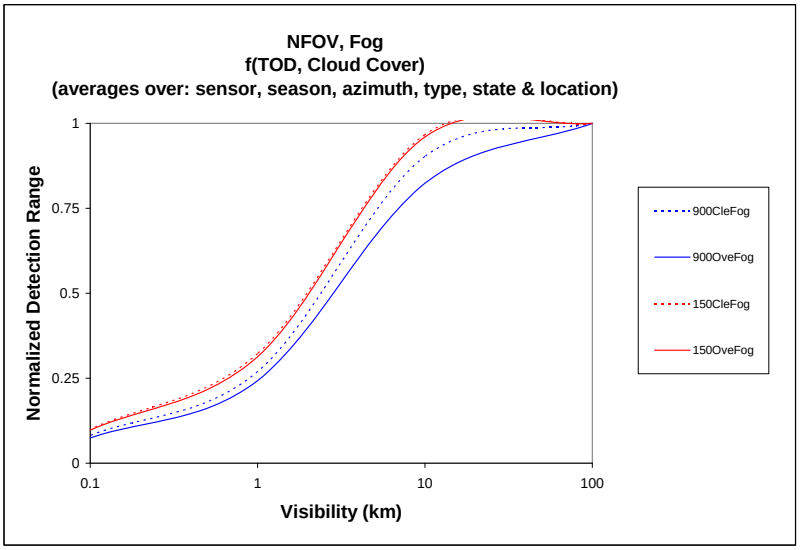

Figure B-1. Normalized detection range vs. visibility for a NFOV average sensor in a fog aerosol as a function of Time of Day (TOD) and, cloud cover. Averages were taken over seasons, locations, azimuths, target types and operating states, as presented in table B-2.

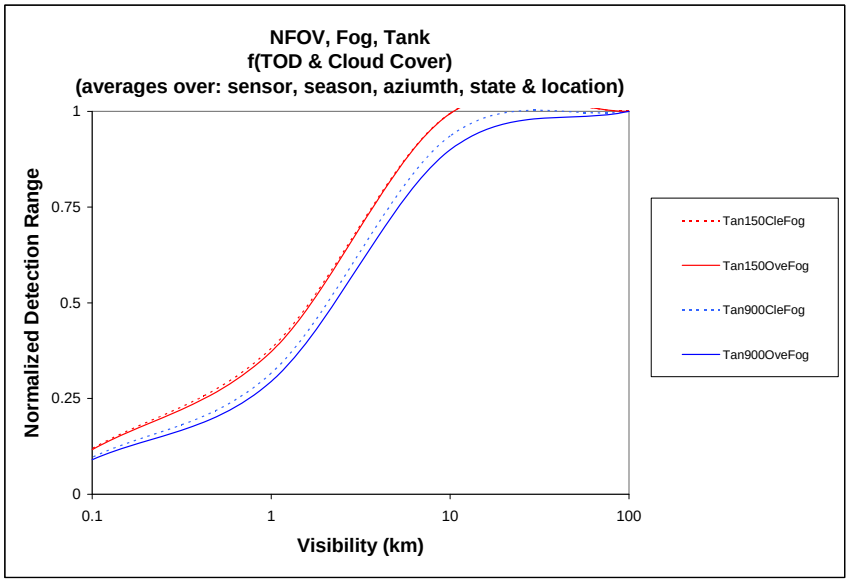

Figure B-2. Normalized detection range vs. visibility for a NFOV average sensor, in a fog aerosol, viewing a tank, as a function of TOD, and cloud cover. Averages were taken over seasons, locations, azimuths, and target operating states, as presented in table B-2.

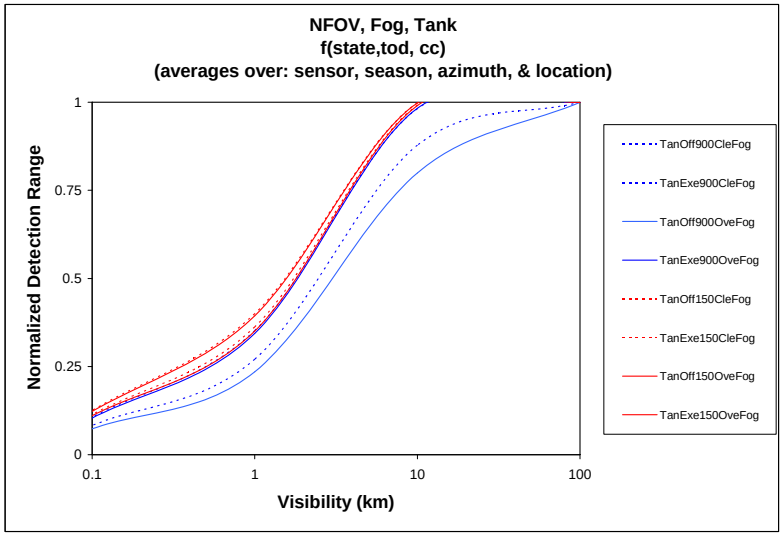

Figure B-3. Normalized detection range vs. visibility for a NFOV average sensor in a fog aerosol as a function of target operating state, TOD, and cloud cover. Averages were taken over seasons, locations, and azimuths, as presented in table B-2.

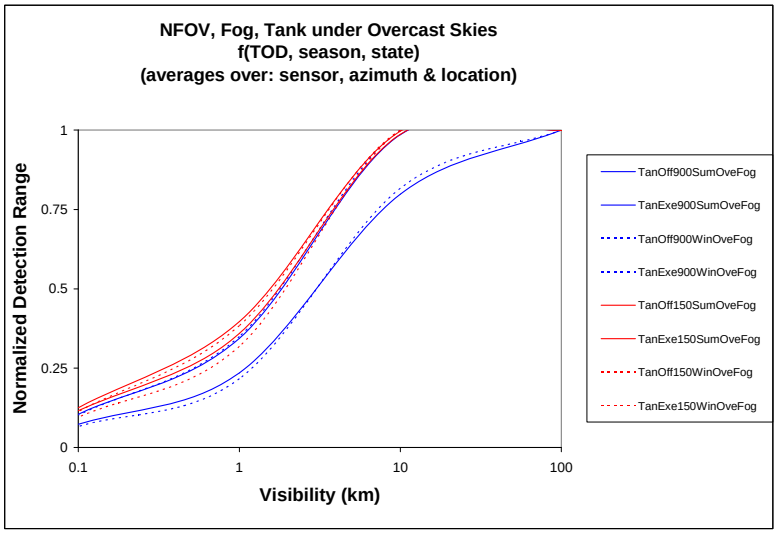

Figure B-4. Normalized detection range vs. visibility for a NFOV average sensor, in a fog aerosol, viewing a tank under overcast skies, as a function of TOD, season, and operating state. Averages were taken over locations, and azimuths, as presented in table B-2.

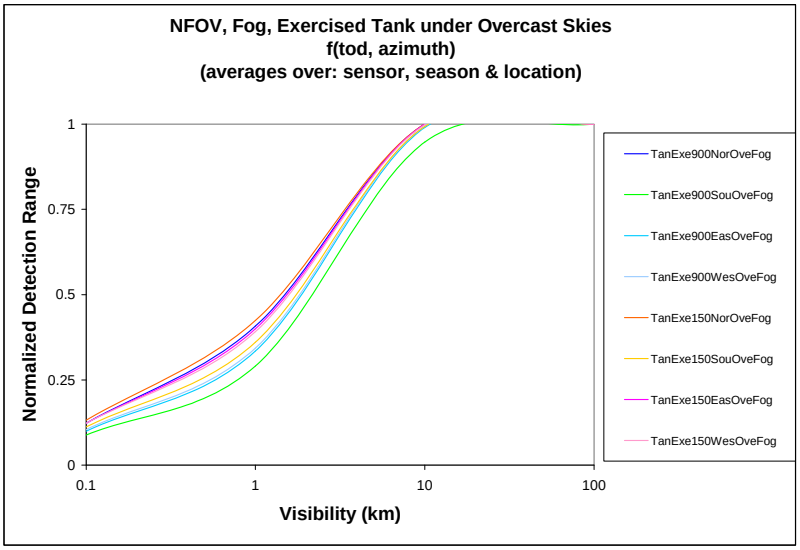

Figure B-5. Normalized detection range vs. visibility for a NFOV average sensor in a fog aerosol viewing an exercised tank under overcast skies as a function of TOD, and azimuth. Averages were taken over seasons and locations, as presented in table B-2.

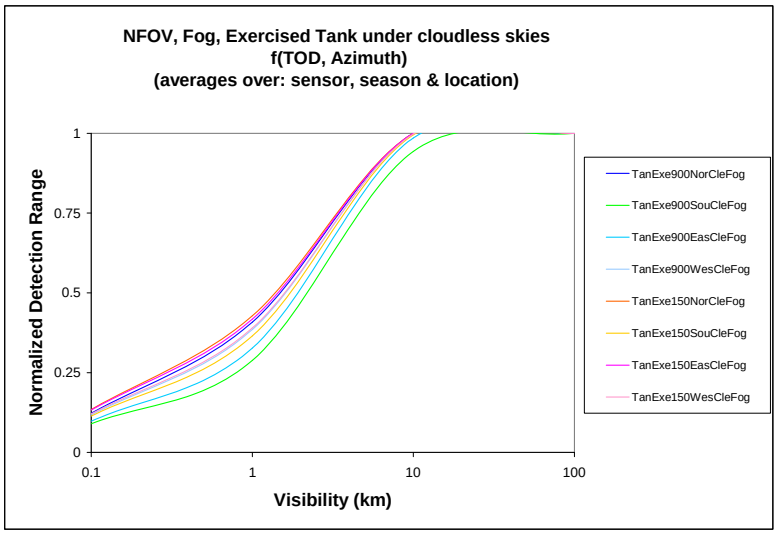

Figure B-6. Normalized detection range vs. visibility for a NFOV average sensor, in a fog aerosol, viewing an exercised tank under clear skies, as a function of TOD, and azimuth. Averages were taken over seasons and locations, as presented in table B-2.

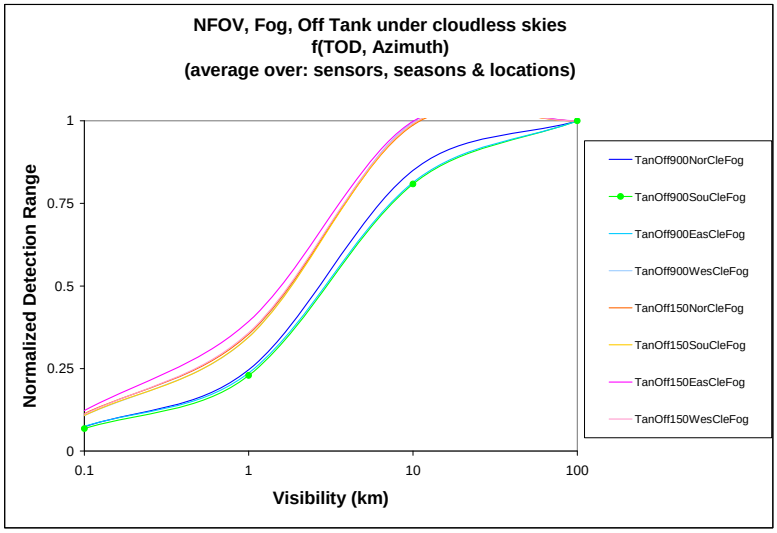

Figure B-7. Normalized detection range vs. visibility for a NFOV average sensor in a fog aerosol viewing an inactive tank under clear skies as a function of TOD, and azimuth. Averages were taken over seasons and locations, as presented in table B-2.

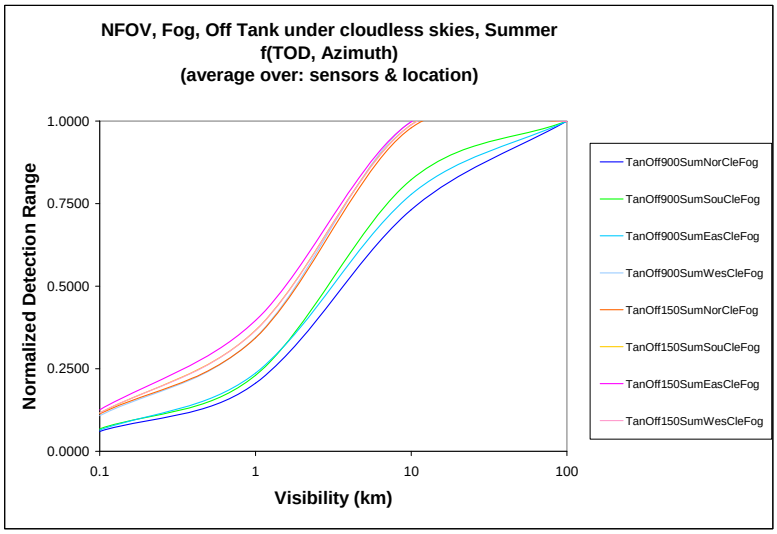

Figure B-8. Normalized detection range vs. visibility for a NFOV average sensor, in a fog aerosol, viewing an inactive tank under clear skies in the summer, as a function of TOD, and azimuth. Averages were taken over locations, as presented in table B-2.

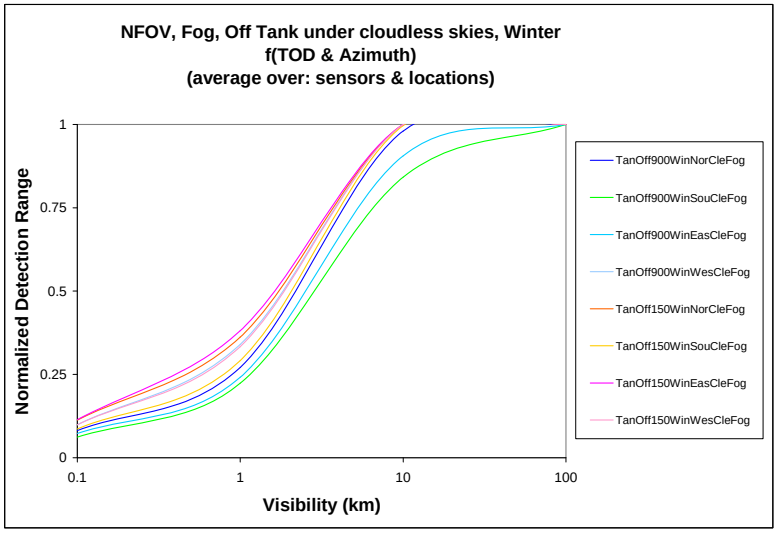

Figure B-9. Normalized detection range vs. visibility for a NFOV average sensor in a fog aerosol viewing an inactive tank under clear skies in the winter as a function of TOD, and azimuth. Averages were taken over locations, as presented in table B-2.

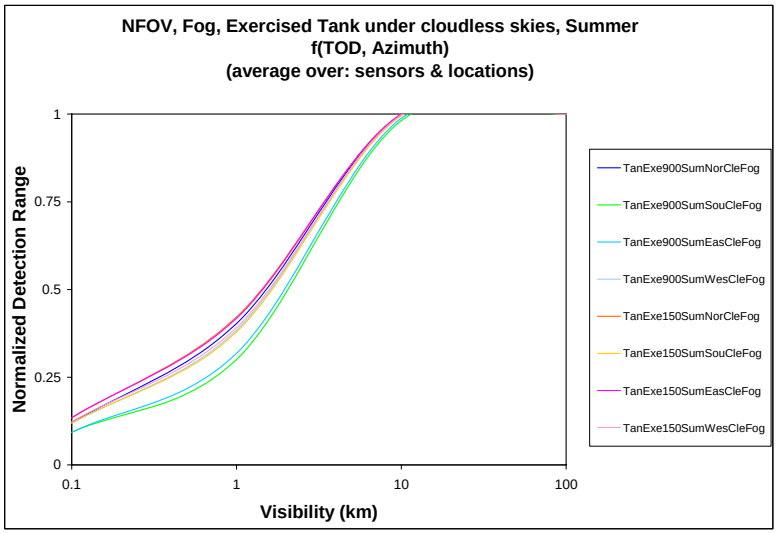

Figure B-10. Normalized detection range vs. visibility for a NFOV average sensor, in a fog aerosol, viewing an exercised tank under clear skies in the summer, as a function of TOD, and azimuth. Averages were taken over locations, as presented in table B-2.

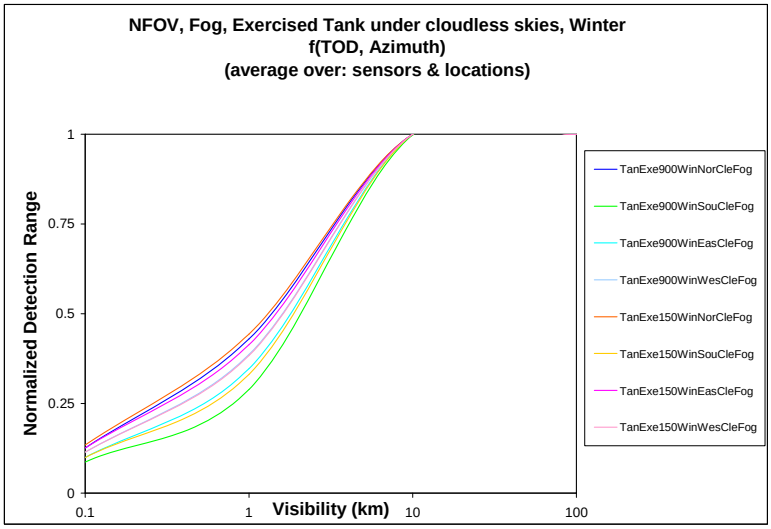

Figure B-11. Normalized detection range vs. visibility for a NFOV average sensor in a fog aerosol viewing an exercised tank under clear skies in the winter as a function of TOD, and azimuth. Averages were taken over locations, as presented in table B-2.

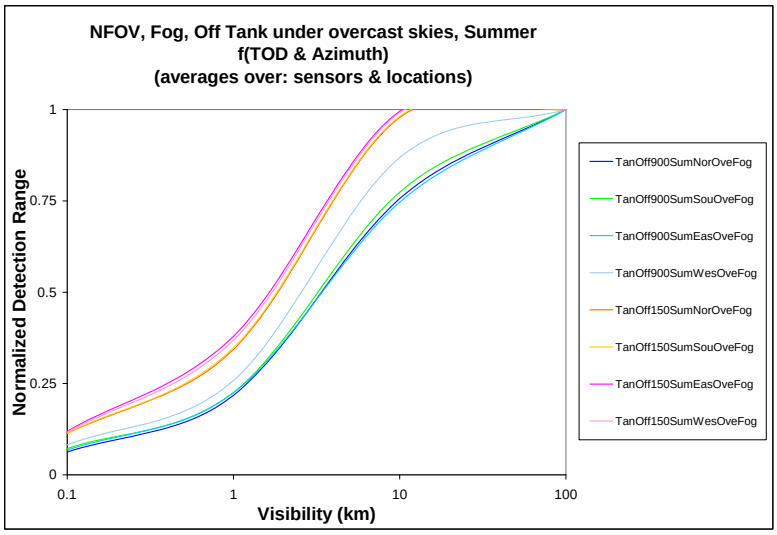

Figure B-12. Normalized detection range vs. visibility for a NFOV average sensor, in a fog aerosol, viewing an inactive tank under overcast skies in the summer, as a function of TOD, and azimuth. Averages were taken over locations, as presented in table B-2.

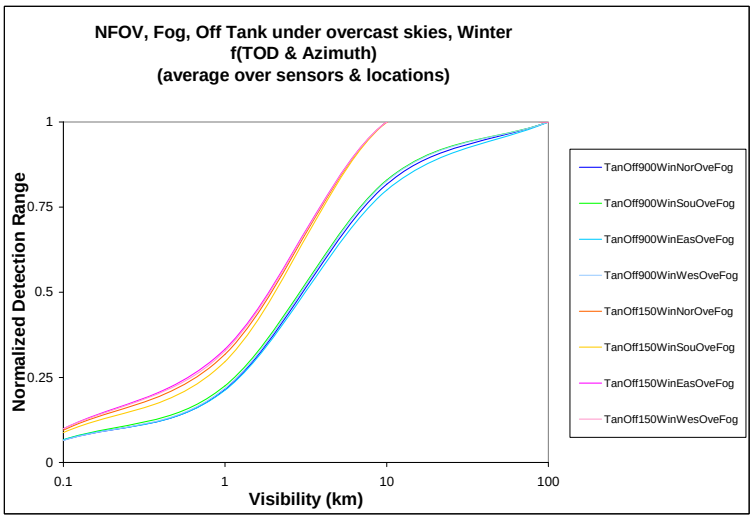

Figure B-13. Normalized detection range vs. visibility for a NFOV average sensor in a fog aerosol viewing an inactive tank under overcast skies in the winter as a function of TOD, and azimuth. Averages were taken over locations, as presented in table B-2.

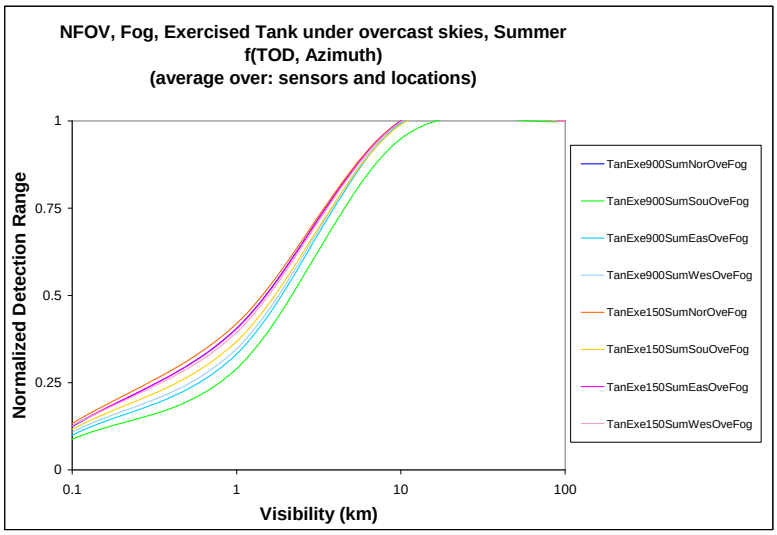

Figure B-14. Normalized detection range vs. visibility for a NFOV average sensor, in a fog aerosol, viewing an exercised tank under overcast skies in the summer, as a function of TOD, and azimuth. Averages were taken over locations, as presented in table B-2.

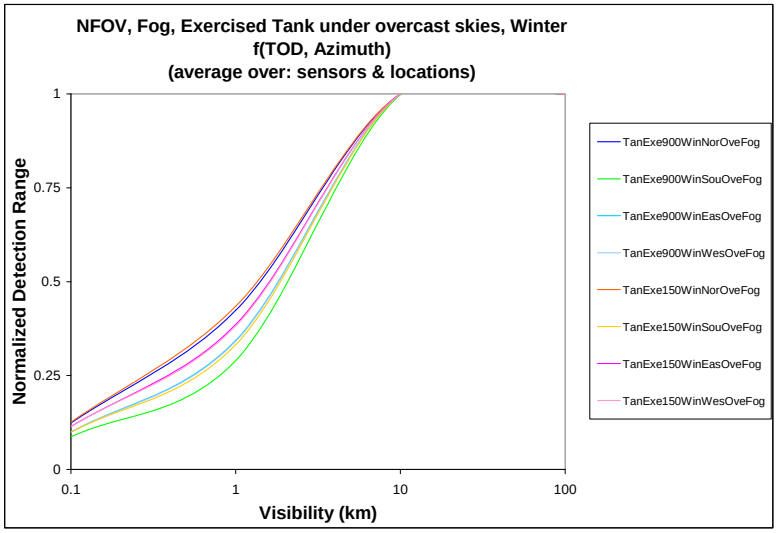

Figure B-15. Normalized detection range vs. visibility for a NFOV average sensor in a fog aerosol viewing an exercised tank under overcast skies in the winter as a function of TOD, and azimuth. Averages were taken over locations, as presented in table B-2.

Appendix C. Third-Order Polynomial Coefficients and Their Curves for the Rural Aerosol for a NFOV and WFOV Average IR Sensor

Table C-1. Third-order polynomial coefficients curve fit to averaged quantities as represented by moniker for and average sensor viewing through a rural aerosol. WFOV results are shown.

Moniker	a0	a1	a2	a3	Average Maximum Detection Range
150CleRur	0.9582	0.0664	-0.0279	0.0034	3.60
150OveRur	0.9540	0.0694	-0.0284	0.0034	3.59
900CleRur	0.8970	0.0915	-0.0268	0.0026	3.48
900OveRur	0.8346	0.1113	-0.0233	0.0015	3.25
Tan900CleRur	0.9456	0.0678	-0.0257	0.0029	2.73
Tan150CleRur	0.9754	0.0477	-0.0219	0.0028	2.80
Tan900OveRur	0.9073	0.0842	-0.0253	0.0025	2.65
Tan150OveRur	0.9747	0.0493	-0.0226	0.0028	2.79
TanExe150OveRur	0.9766	0.0450	-0.0206	0.0026	2.81
TanExe900OveRur	0.9708	0.0573	-0.0262	0.0033	2.78
TanExe150CleRur	0.9772	0.0442	-0.0203	0.0026	2.82
TanExe900CleRur	0.9720	0.0550	-0.0252	0.0032	2.79
TanOff900CleRur	0.9094	0.0854	-0.0263	0.0026	2.65
TanOff150CleRur	0.9736	0.0511	-0.0235	0.0030	2.78
TanOff150OveRur	0.9726	0.0536	-0.0247	0.0031	2.77
TanOff900OveRur	0.8421	0.1118	-0.0243	0.0016	2.51
TanOff900SumOveRur	0.8262	0.1151	-0.0231	0.0014	2.42
TanOff900WinOveRur	0.8216	0.1226	-0.0249	0.0014	2.53
TanOff150SumOveRur	0.9732	0.0505	-0.0231	0.0029	2.77
TanOff150WinOveRur	0.9703	0.0633	-0.0294	0.0037	2.74
TanOff900NorOveRur	0.8016	0.1241	-0.0211	0.0008	2.39
TanOff900EasOveRur	0.8195	0.1172	-0.0226	0.0012	2.39
TanOff900WesOveRur	0.9143	0.0913	-0.0300	0.0031	2.67
TanOff900SouOveRur	0.8290	0.1157	-0.0231	0.0013	2.58
TanExe900SumOveRur	0.9702	0.0575	-0.0263	0.0033	2.78
TanExe900WinOveRur	0.9731	0.0578	-0.0271	0.0034	2.79
TanExe150SumOveRur	0.9764	0.0437	-0.0198	0.0025	2.81
TanExe150WinOveRur	0.9773	0.0487	-0.0229	0.0029	2.81
TanExe900NorOveRur	0.9787	0.0429	-0.0197	0.0025	2.85
TanExe900EasOveRur	0.9713	0.0583	-0.0271	0.0034	2.77
TanExe900WesOveRur	0.9717	0.0571	-0.0264	0.0033	2.78
TanExe900SouOveRur	0.9610	0.0709	-0.0315	0.0039	2.73
TanExe150NorOveRur	0.9792	0.0405	-0.0184	0.0023	2.85
TanExe150EasOveRur	0.9771	0.0433	-0.0198	0.0025	2.82
TanExe150WesOveRur	0.9766	0.0447	-0.0205	0.0026	2.81

Table C-1. Third-order polynomial coefficients curve fit to averaged quantities as represented by moniker for and average sensor viewing through a rural aerosol. WFOV results are shown (continued).

Moniker	a0	a1	a2	a3	Average Maximum Detection Range
TanExe150SouOveRur	0.9736	0.0514	-0.0236	0.0030	2.78
TanExe900NorCleRur	0.9790	0.0424	-0.0195	0.0024	2.85
TanExe900EasCleRur	0.9711	0.0597	-0.0278	0.0035	2.76
TanExe900WesCleRur	0.9762	0.0469	-0.0215	0.0027	2.82
TanExe900SouCleRur	0.9612	0.0712	-0.0317	0.0039	2.72
TanExe150NorCleRur	0.9799	0.0397	-0.0181	0.0023	2.85
TanExe150EasCleRur	0.9781	0.0416	-0.0189	0.0024	2.83
TanExe150WesCleRur	0.9768	0.0453	-0.0210	0.0027	2.80
TanExe150SouCleRur	0.9740	0.0503	-0.0231	0.0029	2.79
TanOff900NorCleRur	0.8869	0.0970	-0.0263	0.0023	2.69
TanOff900EasCleRur	0.8805	0.0988	-0.0263	0.0023	2.61
TanOff900WesCleRur	0.9715	0.0555	-0.0253	0.0032	2.79
TanOff900SouCleRur	0.8682	0.1051	-0.0274	0.0023	2.49
TanOff150NorCleRur	0.9729	0.0520	-0.0239	0.0030	2.78
TanOff150EasCleRur	0.9764	0.0450	-0.0205	0.0026	2.81
TanOff150WesCleRur	0.9733	0.0525	-0.0243	0.0031	2.77
TanOff150SouCleRur	0.9717	0.0549	-0.0253	0.0032	2.77
TanOff900SumNorCleRur	0.7072	0.1484	-0.0085	-0.0022	2.62
TanOff900SumEasCleRur	0.7828	0.1273	-0.0180	0.0001	2.84
TanOff900SumWesCleRur	0.9716	0.0560	-0.0254	0.0032	2.78
TanOff900SumSouCleRur	0.8965	0.0971	-0.0287	0.0027	2.71
TanOff150SumNorCleRur	0.9723	0.0531	-0.0245	0.0031	2.76
TanOff150SumEasCleRur	0.9763	0.0442	-0.0200	0.0025	2.81
TanOff150SumWesCleRur	0.9739	0.0502	-0.0232	0.0029	2.78
TanOff150SumSouCleRur	0.9740	0.0489	-0.0222	0.0028	2.78
TanOff900WinNorCleRur	0.9574	0.0772	-0.0341	0.0042	2.74
TanOff90Win0EasCleRur	0.9161	0.0918	-0.0312	0.0033	2.70
TanOff900WinWesCleRur	0.9706	0.0589	-0.0271	0.0034	2.80
TanOff900WinSouCleRur	0.8650	0.1096	-0.0306	0.0029	2.44
TanOff150WinNorCleRur	0.9735	0.0516	-0.0236	0.0030	2.83
TanOff150WinEasCleRur	0.9764	0.0480	-0.0223	0.0028	2.81
TanOff150WinWesCleRur	0.9714	0.0604	-0.0280	0.0035	2.76
TanOff150WinSouCleRur	0.9649	0.0705	-0.0326	0.0041	2.74
TanExe900SumNorCleRur	0.9782	0.0434	-0.0199	0.0025	2.85
TanExe900SumEasCleRur	0.9695	0.0616	-0.0287	0.0036	2.75
TanExe900SumWesCleRur	0.9762	0.0468	-0.0215	0.0027	2.81
TanExe900SumSouCleRur	0.9671	0.0658	-0.0302	0.0038	2.74
TanExe150SumNorCleRur	0.9778	0.0410	-0.0183	0.0023	2.85
TanExe150SumEasCleRur	0.9772	0.0413	-0.0186	0.0023	2.83
TanExe150SumWesCleRur	0.9764	0.0446	-0.0206	0.0026	2.80
TanExe150SumSouCleRur	0.9747	0.0464	-0.0211	0.0027	2.81
TanExe900WinNorCleRur	0.9837	0.0395	-0.0191	0.0025	2.85
TanExe90Win0EasCleRur	0.9741	0.0566	-0.0265	0.0033	2.78
TanExe900WinWesCleRur	0.9764	0.0477	-0.0223	0.0028	2.85

Table C-1. Third-order polynomial coefficients curve fit to averaged quantities as represented by moniker for and average sensor viewing through a rural aerosol. WFOV results are shown (continued).

Moniker	a0	a1	a2	a3	Average Maximum Detection Range
TanExe900WinSouCleRur	0.9645	0.0736	-0.0340	0.0043	2.74
TanExe150WinNorCleRur	0.9852	0.0370	-0.0180	0.0023	2.85
TanExe150WinEasCleRur	0.9796	0.0427	-0.0199	0.0025	2.85
TanExe150WinWesCleRur	0.9774	0.0483	-0.0228	0.0029	2.81
TanExe150WinSouCleRur	0.9721	0.0603	-0.0281	0.0035	2.76
TanOff900SumNorOveRur	0.7385	0.1382	-0.0148	-0.0006	2.20
TanOff900SumEasOveRur	0.7629	0.1332	-0.0180	0.0001	2.10
TanOff900SumWesOveRur	0.9414	0.0825	-0.0323	0.0037	2.68
TanOff900SumSouOveRur	0.8291	0.1148	-0.0243	0.0016	2.62
TanOff150SumNorOveRur	0.9717	0.0543	-0.0250	0.0032	2.75
TanOff150SumEasOveRur	0.9750	0.0467	-0.0212	0.0026	2.79
TanOff150SumWesOveRur	0.9739	0.0486	-0.0222	0.0028	2.78
TanOff150SumSouOveRur	0.9720	0.0526	-0.0241	0.0030	2.77
TanOff900WinNorOveRur	0.8006	0.1269	-0.0239	0.0013	2.47
TanOff900Win0EasOveRu	0.8508	0.1136	-0.0279	0.0022	2.56
TanOff900WinWesOveRur	0.8532	0.1159	-0.0270	0.0019	2.63
TanOff900WinSouOveRur	0.7820	0.1339	-0.0205	0.0004	2.45
TanOff150WinNorOveRur	0.9701	0.0626	-0.0289	0.0036	2.74
TanOff150WinEasOveRur	0.9727	0.0599	-0.0281	0.0035	2.74
TanOff150WinWesOveRur	0.9715	0.0611	-0.0284	0.0036	2.74
TanOff150WinSouOveRur	0.9667	0.0698	-0.0321	0.0040	2.73
TanExe900SumNorOveRur	0.9782	0.0434	-0.0199	0.0025	2.85
TanExe900SumEasOveRur	0.9697	0.0603	-0.0280	0.0035	2.77
TanExe900SumWesOveRur	0.9723	0.0554	-0.0255	0.0032	2.78
TanExe900SumSouOveRur	0.9600	0.0713	-0.0317	0.0039	2.72
TanExe150SumNorOveRur	0.9777	0.0412	-0.0184	0.0023	2.85
TanExe150SumEasOveRur	0.9774	0.0414	-0.0187	0.0023	2.81
TanExe150SumWesOveRur	0.9764	0.0434	-0.0198	0.0025	2.81
TanExe150SumSouOveRur	0.9739	0.0486	-0.0222	0.0028	2.78
TanExe900WinNorOveRur	0.9828	0.0403	-0.0193	0.0025	2.85
TanExe900WinEasOveRur	0.9727	0.0578	-0.0271	0.0034	2.78
TanExe900WinWesOveRur	0.9717	0.0604	-0.0283	0.0036	2.78
TanExe900WinSouOveRur	0.9644	0.0728	-0.0335	0.0042	2.75
TanExe150WinNorOveRur	0.9832	0.0393	-0.0188	0.0024	2.85
TanExe150WinEasOveRur	0.9772	0.0475	-0.0222	0.0028	2.81
TanExe150WinWesOveRur	0.9769	0.0484	-0.0227	0.0029	2.81
TanExe150WinSouOveRur	0.9718	0.0597	-0.0277	0.0035	2.77

Table C-2. Third-order polynomial coefficients curve fit to averaged quantities as represented by moniker for an average sensor viewing through a rural aerosol. NFOV results are shown. Coefficients in blue have associated curves presented in the graphs in this appendix.

Moniker	a0	a1	a2	a3	Average Maximum Detection Range
150CleRur	0.8336	0.1492	-0.0400	0.0033	8.88
150OveRur	0.8187	0.1529	-0.0378	0.0029	8.88
900CleRur	0.7362	0.1679	-0.0276	0.0008	8.65
900OveRur	0.6396	0.1812	-0.0143	-0.0018	8.12
Tan900CleRur	0.8115	0.1505	-0.0369	0.0028	7.67
Tan150CleRur	0.8913	0.1320	-0.0462	0.0049	7.80
Tan900OveRur	0.7347	0.1652	-0.0264	0.0007	7.50
Tan150OveRur	0.8832	0.1345	-0.0453	0.0047	7.80
TanExe150OveRur	0.9061	0.1280	-0.0481	0.0054	7.80
TanExe900OveRur	0.8552	0.1434	-0.0425	0.0039	7.80
TanExe150CleRur	0.9103	0.1264	-0.0484	0.0055	7.80
TanExe900CleRur	0.8657	0.1399	-0.0436	0.0043	7.80
TanOff900CleRur	0.7399	0.1643	-0.0280	0.0010	7.49
TanOff150CleRur	0.8723	0.1376	-0.0440	0.0044	7.80
TanOff150OveRur	0.8604	0.1409	-0.0426	0.0040	7.80
TanOff900OveRur	0.6085	0.1864	-0.0099	-0.0026	7.18
TanOff900SumOveRur	0.5971	0.1860	-0.0091	-0.0027	6.98
TanOff900WinOveRur	0.5940	0.1951	-0.0080	-0.0033	7.57
TanOff150SumOveRur	0.8554	0.1405	-0.0410	0.0037	7.80
TanOff150WinOveRur	0.8677	0.1439	-0.0462	0.0046	7.80
TanOff900NorOveRur	0.5746	0.1902	-0.0058	-0.0034	6.91
TanOff900EasOveRur	0.5900	0.1833	-0.0085	-0.0026	6.63
TanOff900WesOveRur	0.6787	0.1816	-0.0180	-0.0014	7.78
TanOff900SouOveRur	0.5854	0.1907	-0.0069	-0.0033	7.36
TanExe900SumOveRur	0.8563	0.1431	-0.0426	0.0040	7.80
TanExe900WinOveRur	0.8926	0.1371	-0.0493	0.0053	7.80
TanExe150SumOveRur	0.8961	0.1295	-0.0461	0.0050	7.80
TanExe150WinOveRur	0.9318	0.1248	-0.0535	0.0064	7.80
TanExe900NorOveRur	0.9308	0.1224	-0.0519	0.0062	7.80
TanExe900EasOveRur	0.8494	0.1457	-0.0422	0.0038	7.80
TanExe900WesOveRur	0.8663	0.1412	-0.0444	0.0043	7.80
TanExe900SouOveRur	0.7741	0.1638	-0.0315	0.0014	7.80
TanExe150NorOveRur	0.9269	0.1207	-0.0499	0.0059	7.80
TanExe150EasOveRur	0.9138	0.1259	-0.0491	0.0056	7.80
TanExe150WesOveRur	0.9068	0.1279	-0.0482	0.0054	7.80
TanExe150SouOveRur	0.8770	0.1374	-0.0452	0.0046	7.80
TanExe900NorCleRur	0.9315	0.1221	-0.0519	0.0062	7.80
TanExe900EasCleRur	0.8406	0.1475	-0.0407	0.0035	7.80
TanExe900WesCleRur	0.9186	0.1264	-0.0507	0.0059	7.80
TanExe900SouCleRur	0.7718	0.1632	-0.0313	0.0014	7.80
TanExe150NorCleRur	0.9282	0.1202	-0.0500	0.0059	7.80
TanExe150EasCleRur	0.9241	0.1216	-0.0496	0.0058	7.80
TanExe150WesCleRur	0.9051	0.1283	-0.0480	0.0053	7.80

Table C-2. Third-order polynomial coefficients curve fit to averaged quantities as represented by moniker for an average sensor viewing through a rural aerosol. NFOV results are shown. Coefficients in blue have associated curves presented in the graphs in this appendix (continued).

Moniker	a0	a1	a2	a3	Average Maximum Detection Range
TanExe150SouCleRur	0.8839	0.1354	-0.0460	0.0048	7.80
TanOff900NorCleRur	0.6740	0.1789	-0.0186	-0.0011	7.84
TanOff900EasCleRur	0.7214	0.1681	-0.0258	0.0005	7.19
TanOff900WesCleRur	0.8778	0.1388	-0.0462	0.0047	7.80
TanOff900SouCleRur	0.6381	0.1795	-0.0154	-0.0014	7.03
TanOff150NorCleRur	0.8639	0.1399	-0.0430	0.0041	7.80
TanOff150EasCleRur	0.9089	0.1273	-0.0485	0.0055	7.80
TanOff150WesCleRur	0.8697	0.1387	-0.0439	0.0043	7.80
TanOff150SouCleRur	0.8467	0.1443	-0.0407	0.0036	7.80
TanOff900SumNorCleRur	0.4846	0.2042	0.0064	-0.0057	8.05
TanOff900SumEasCleRur	0.5682	0.2018	-0.0033	-0.0044	8.34
TanOff900SumWesCleRur	0.8754	0.1394	-0.0459	0.0047	7.80
TanOff900SumSouCleRur	0.6589	0.1820	-0.0164	-0.0015	7.74
TanOff150SumNorCleRur	0.8315	0.1464	-0.0376	0.0030	7.80
TanOff150SumEasCleRur	0.8986	0.1284	-0.0463	0.0050	7.80
TanOff150SumWesCleRur	0.8620	0.1390	-0.0419	0.0040	7.80
TanOff150SumSouCleRur	0.8655	0.1384	-0.0426	0.0041	7.80
TanOff900WinNorCleRur	0.7827	0.1641	-0.0340	0.0019	7.80
TanOff90Win0EasCleRur	0.7223	0.1775	-0.0251	-0.0001	7.80
TanOff900WinWesCleRur	0.9160	0.1335	-0.0539	0.0063	7.80
TanOff900WinSouCleRur	0.6477	0.1778	-0.0185	-0.0008	6.87
TanOff150WinNorCleRur	0.9293	0.1277	-0.0544	0.0065	7.80
TanOff150WinEasCleRur	0.9381	0.1242	-0.0549	0.0067	7.80
TanOff150WinWesCleRur	0.8928	0.1378	-0.0498	0.0054	7.80
TanOff150WinSouCleRur	0.8095	0.1579	-0.0378	0.0027	7.80
TanExe900SumNorCleRur	0.9349	0.1223	-0.0530	0.0064	7.80
TanExe900SumEasCleRur	0.8188	0.1525	-0.0375	0.0028	7.80
TanExe900SumWesCleRur	0.9208	0.1260	-0.0511	0.0060	7.80
TanExe900SumSouCleRur	0.8008	0.1573	-0.0352	0.0023	7.80
TanExe150SumNorCleRur	0.9190	0.1224	-0.0486	0.0056	7.80
TanExe150SumEasCleRur	0.9143	0.1231	-0.0477	0.0054	7.80
TanExe150SumWesCleRur	0.8938	0.1301	-0.0459	0.0049	7.80
TanExe150SumSouCleRur	0.8852	0.1332	-0.0452	0.0047	7.80
TanExe900WinNorCleRur	0.9523	0.1160	-0.0544	0.0068	7.80
TanExe90Win0EasCleRur	0.9215	0.1307	-0.0539	0.0063	7.80
TanExe900WinWesCleRur	0.9437	0.1220	-0.0553	0.0068	7.80
TanExe900WinSouCleRur	0.8124	0.1580	-0.0387	0.0029	7.80
TanExe150WinNorCleRur	0.9531	0.1147	-0.0539	0.0068	7.80
TanExe150WinEasCleRur	0.9487	0.1185	-0.0548	0.0068	7.80
TanExe150WinWesCleRur	0.9389	0.1229	-0.0544	0.0066	7.80
TanExe150WinSouCleRur	0.8895	0.1391	-0.0496	0.0053	7.80
TanOff900SumNorOveRur	0.5360	0.1896	-0.0022	-0.0037	6.87
TanOff900SumEasOveRur	0.5363	0.1841	-0.0027	-0.0034	5.73
TanOff900SumWesOveRur	0.7051	0.1792	-0.0215	-0.0008	7.80

Table C-2. Third-order polynomial coefficients curve fit to averaged quantities as represented by moniker for an average sensor viewing through a rural aerosol. NFOV results are shown. Coefficients in blue have associated curves presented in the graphs in this appendix (continued).

Moniker	a0	a1	a2	a3	Average Maximum Detection Range
TanOff900SumSouOveRur	0.5804	0.1914	-0.0068	-0.0032	7.38
TanOff150SumNorOveRur	0.8304	0.1466	-0.0375	0.0030	7.80
TanOff150SumEasOveRur	0.8864	0.1325	-0.0451	0.0047	7.80
TanOff150SumWesOveRur	0.8664	0.1380	-0.0426	0.0041	7.80
TanOff150SumSouOveRur	0.8385	0.1447	-0.0386	0.0032	7.80
TanOff900WinNorOveRur	0.5750	0.2012	-0.0044	-0.0042	7.53
TanOff900Win0EasOveRu	0.6146	0.1897	-0.0114	-0.0025	7.52
TanOff900WinWesOveRur	0.6301	0.1856	-0.0134	-0.0021	7.72
TanOff900WinSouOveRur	0.5527	0.2039	-0.0024	-0.0045	7.49
TanOff150WinNorOveRur	0.8636	0.1447	-0.0455	0.0044	7.80
TanOff150WinEasOveRur	0.8982	0.1365	-0.0506	0.0056	7.80
TanOff150WinWesOveRur	0.8884	0.1388	-0.0491	0.0053	7.80
TanOff150WinSouOveRur	0.8206	0.1556	-0.0396	0.0031	7.80
TanExe900SumNorOveRur	0.9352	0.1217	-0.0528	0.0064	7.80
TanExe900SumEasOveRur	0.8419	0.1475	-0.0411	0.0036	7.80
TanExe900SumWesOveRur	0.8765	0.1387	-0.0458	0.0047	7.80
TanExe900SumSouOveRur	0.7716	0.1641	-0.0310	0.0013	7.80
TanExe150SumNorOveRur	0.9173	0.1229	-0.0484	0.0056	7.80
TanExe150SumEasOveRur	0.9054	0.1269	-0.0473	0.0053	7.80
TanExe150SumWesOveRur	0.8961	0.1297	-0.0463	0.0050	7.80
TanExe150SumSouOveRur	0.8655	0.1384	-0.0426	0.0041	7.80
TanExe900WinNorOveRur	0.9510	0.1171	-0.0546	0.0068	7.80
TanExe900WinEasOveRur	0.9065	0.1360	-0.0526	0.0060	7.80
TanExe900WinWesOveRur	0.8995	0.1372	-0.0513	0.0057	7.80
TanExe900WinSouOveRur	0.8134	0.1579	-0.0389	0.0029	7.80
TanExe150WinNorOveRur	0.9517	0.1158	-0.0541	0.0068	7.80
TanExe150WinEasOveRur	0.9398	0.1225	-0.0545	0.0067	7.80
TanExe150WinWesOveRur	0.9369	0.1237	-0.0543	0.0066	7.80
TanExe150WinSouOveRur	0.8986	0.1370	-0.0510	0.0056	7.80

The coefficients displayed in blue in table C-2 have associated curves that are presented in the following graphs labeled figures C-1 through C-15.

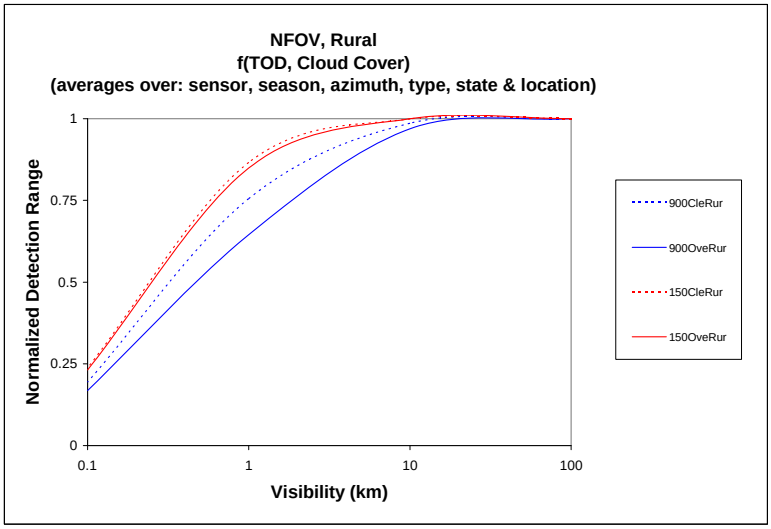

Figure C-1. Normalized detection range vs. visibility for a NFOV average sensor in a rural aerosol as a function of TOD, and cloud cover. Averages were taken over seasons, locations, azimuths, target types and operating states, as presented in table C-2.

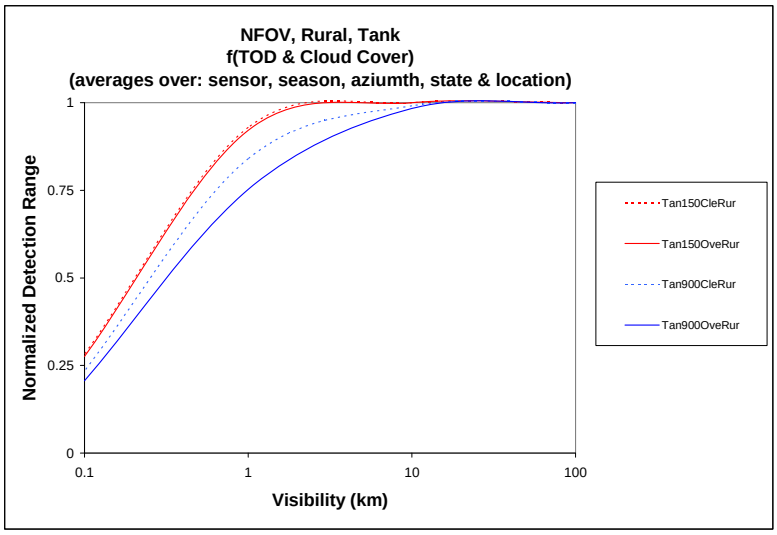

Figure C-2. Normalized detection range vs. visibility for a NFOV average sensor, in a rural aerosol, viewing a tank, as a function of TOD, and cloud cover. Averages were taken over seasons, locations, azimuths, and target operating states, as presented in table C-2.

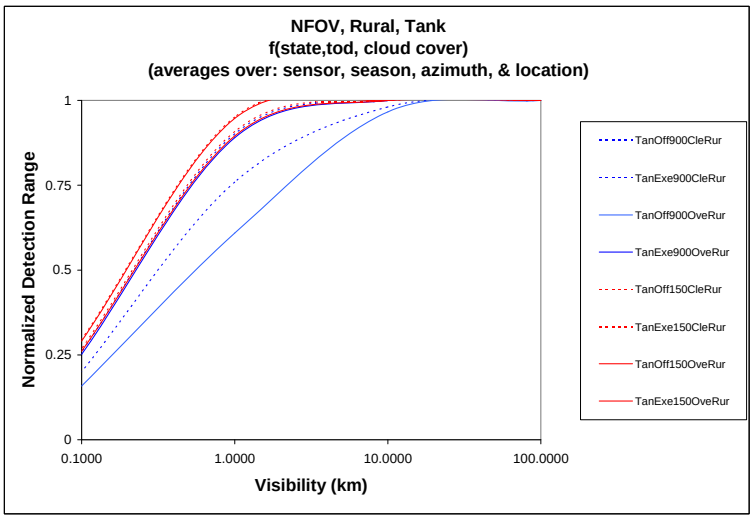

Figure C-3. Normalized detection range vs. visibility for a NFOV average sensor in a rural aerosol as a function of target operating state, TOD, and cloud cover. Averages were taken over seasons, locations, and azimuths, as presented in table C-2.

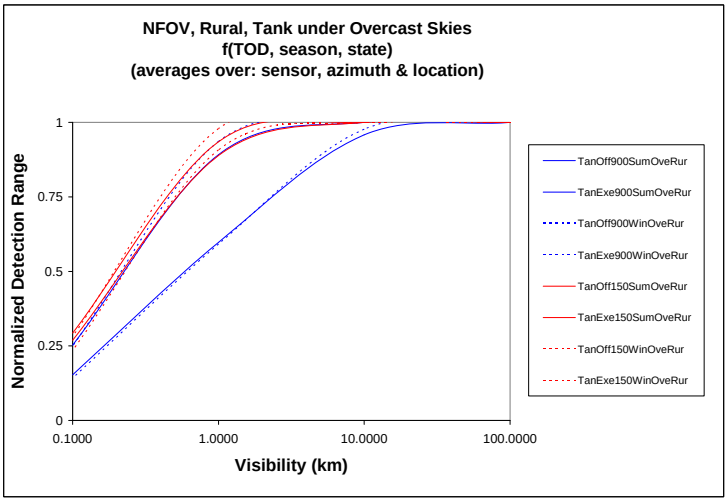

Figure C-4. Normalized detection range vs. visibility for a NFOV average sensor, in a rural aerosol, viewing a tank under overcast skies, as a function of TOD, season, and operating state. Averages were taken over locations, and azimuths, as presented in table C-2.

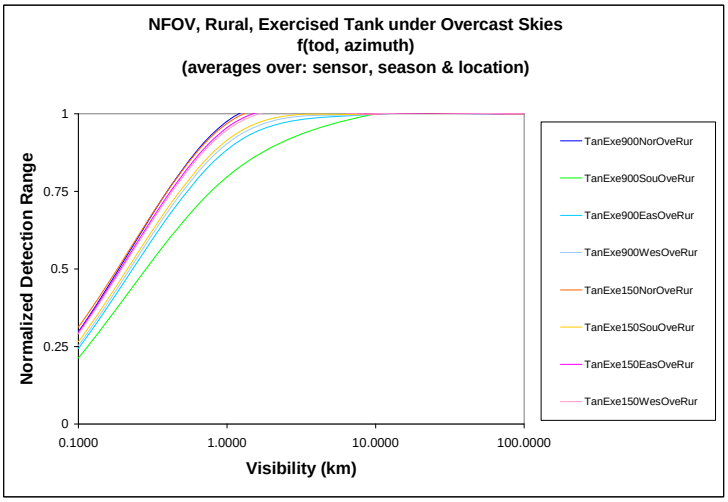

Figure C-5. Normalized detection range vs. visibility for a NFOV average sensor in a rural aerosol viewing an exercised tank under overcast skies as a function of TOD, and azimuth. Averages were taken over seasons and locations, as presented in table C-2.

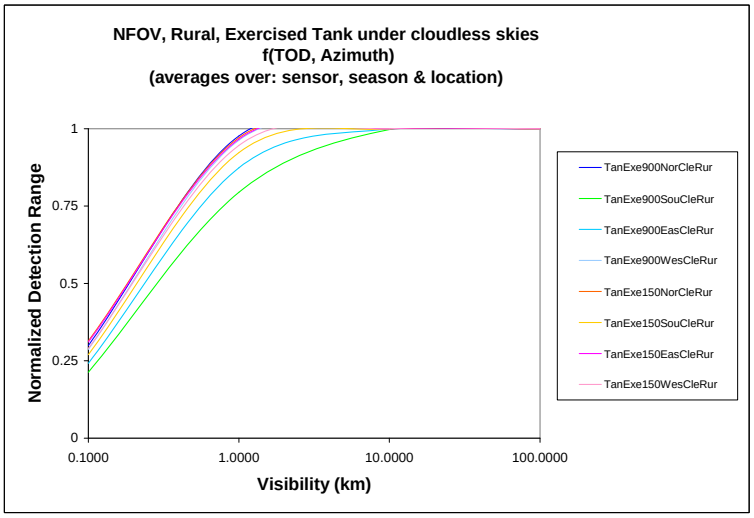

Figure C-6. Normalized detection range vs. visibility for a NFOV average sensor, in a rural aerosol, viewing an exercised tank under clear skies, as a function of TOD, and azimuth. Averages were taken over seasons and locations, as presented in table C-2.

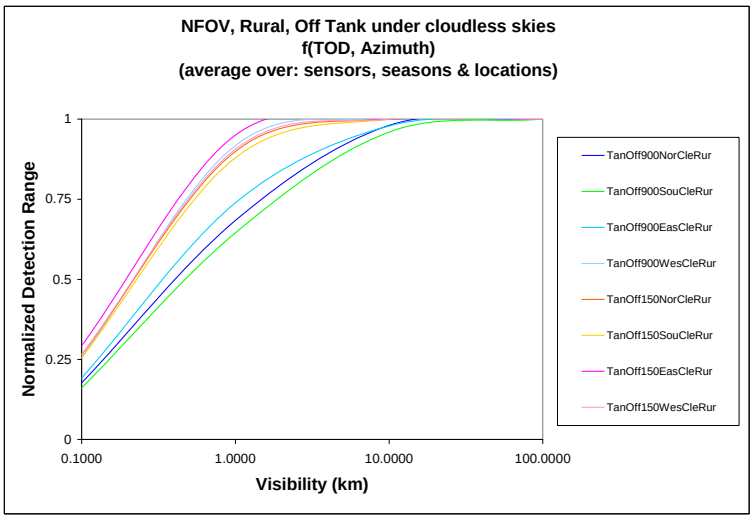

Figure C-7. Normalized detection range vs. visibility for a NFOV average sensor in a rural aerosol viewing an inactive tank under clear skies as a function of TOD, and azimuth. Averages were taken over seasons and locations, as presented in table C-2.

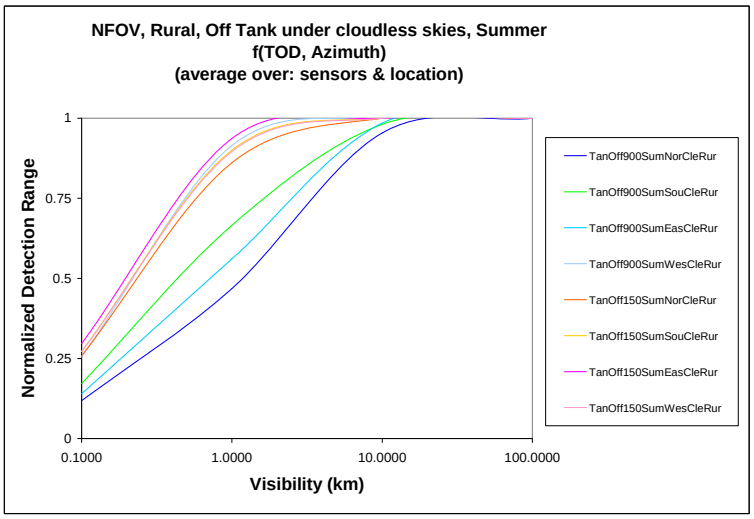

Figure C-8. Normalized detection range vs. visibility for a NFOV average sensor, in a rural aerosol, viewing an inactive tank under clear skies in the summer, as a function of TOD, and azimuth. Averages were taken over locations, as presented in table C-2.

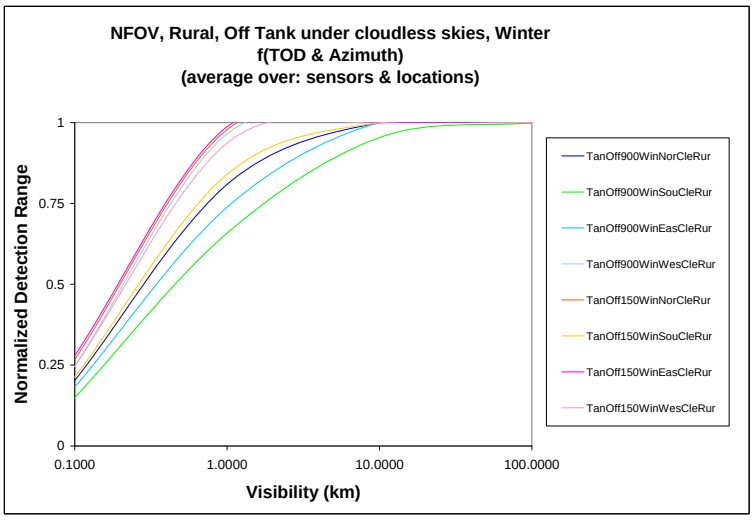

Figure C-9. Normalized detection range vs. visibility for a NFOV average sensor in a rural aerosol viewing an inactive tank under clear skies in the winter as a function of TOD, and azimuth. Averages were taken over locations, as presented in table C-2.

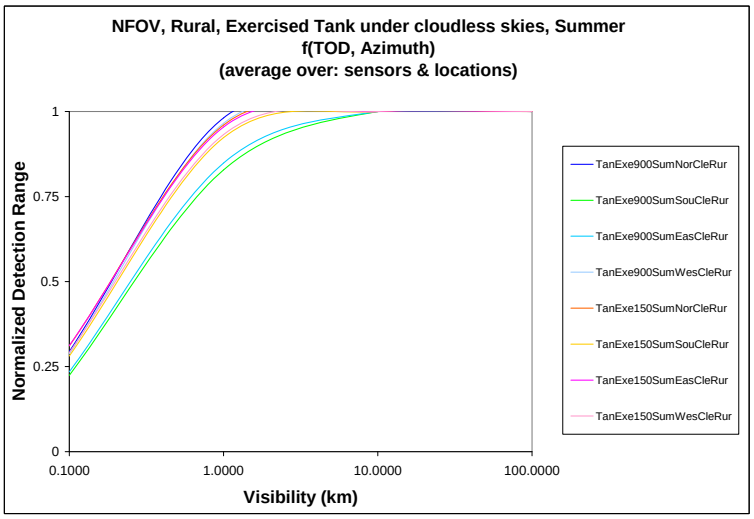

Figure C-10. Normalized detection range vs. visibility for a NFOV average sensor, in a rural aerosol, viewing an exercised tank under clear skies in the summer, as a function of TOD, and azimuth. Averages were taken over locations, as presented in table C-2.

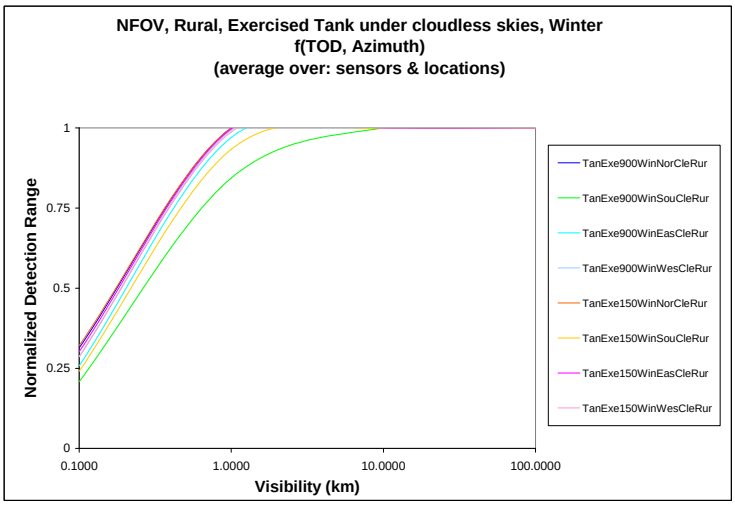

Figure C-11. Normalized detection range vs. visibility for a NFOV average sensor in a rural aerosol viewing an exercised tank under clear skies in the winter as a function of TOD, and azimuth. Averages were taken over locations, as presented in table c-2.

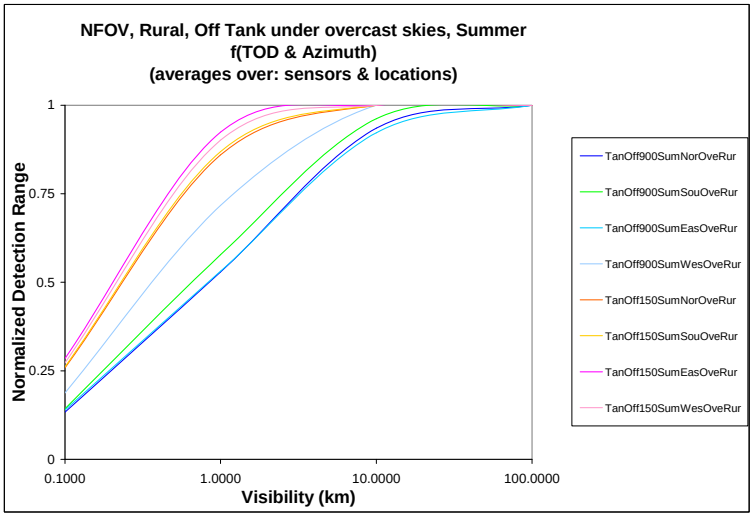

Figure C-12. Normalized detection range vs. visibility for a NFOV average sensor, in a rural aerosol, viewing an inactive tank under overcast skies in the summer, as a function of TOD, and azimuth. Averages were taken over locations, as presented in table C-2.

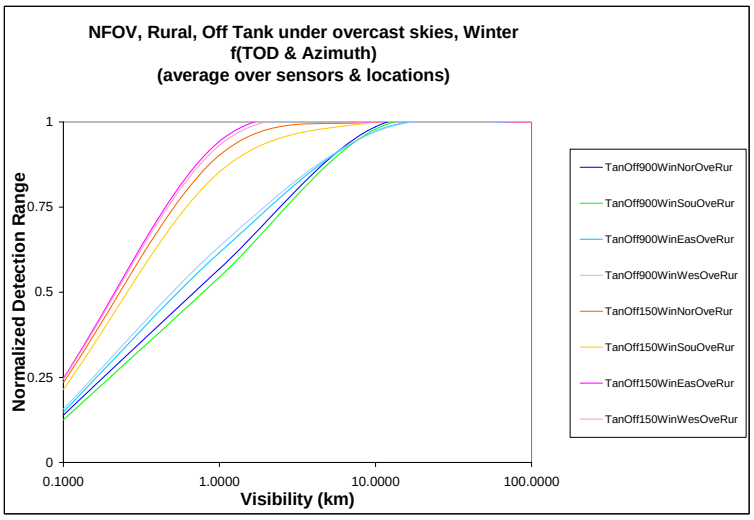

Figure C-13. Normalized detection range vs. visibility for a NFOV average sensor in a rural aerosol viewing an inactive tank under overcast skies in the winter as a function of TOD, and azimuth. Averages were taken over locations, as presented in table C-2.

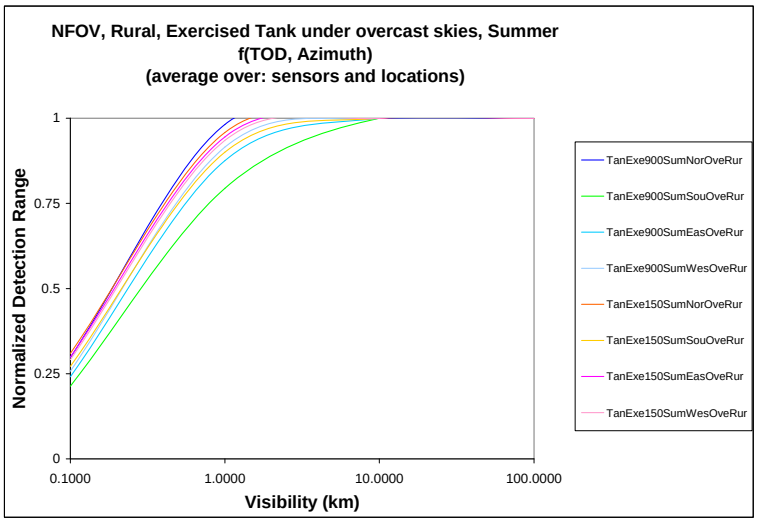

Figure C-14. Normalized detection range vs. visibility for a NFOV average sensor, in a rural aerosol, viewing an exercised tank under overcast skies in the summer, as a function of TOD, and azimuth. Averages were taken over locations, as presented in table C-2.

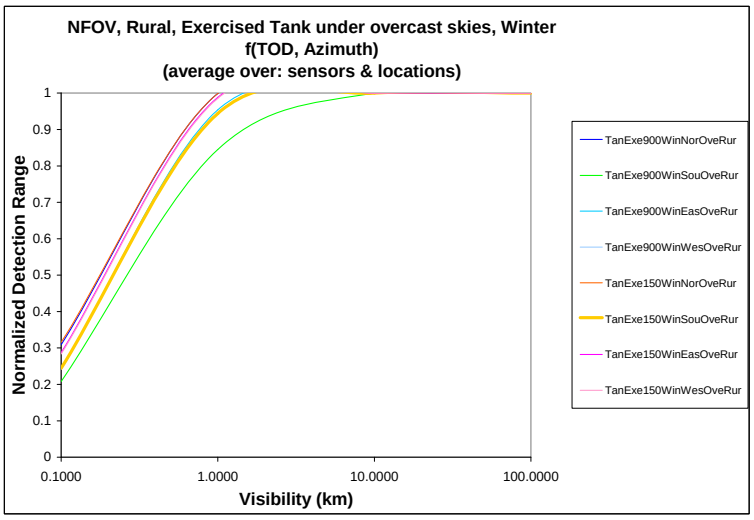

Figure C-15. Normalized detection range vs. visibility for a NFOV average sensor in a rural aerosol viewing an exercised tank under overcast skies in the winter as a function of TOD, and azimuth. Averages were taken over locations, as presented in table C-2.

References

1. O'Brien, S. G.; Shirkey, R. C. *Adding Weather to Wargames*; ARL-TR-4005; U.S. Army Research Laboratory: White Sands Missile Range, NM, January 2007.

2. Press, W. H.; Teukolsky, S. A.; Vetterling, W. T.; Flannery, B. P. *Numerical Recipes in Fortran 77: the art of scientific computing*; 2nd ed, pp 678*ff*, Cambridge University Press: New York, NY, 2003.

No. Copies	Organization
1	Army Research Laboratory Attn: AMSRD-ARL-CI-EE (Dr. Hoock) WSMR NM 88002-5501
2	Army Research Laboratory Attn: AMSRD-ARL-CI-EE (Dr. Shirkey) WSMR NM 88002-5501
2	Army Research Laboratory Attn: AMSRD-ARL-CI-EE (Dr. O'Brien) WSMR NM 88002-5501
1	Director, USA TRADOC Analysis Center Attn: ATRC-WEC (D. Durda) WSMR, NM 88002-5502
1	Army Research Laboratory Attn: AMSRD-ARL-RO-EN (Dr. Bach) PO Box 12211 Research Triangle Park, NC 27009
1	Army Materiel Systems Analysis Activity Attn: AMXSY-SC (J. Mazz) 392 Hopkins Road APG MD 21005-5071
1	Army Materiel Systems Analysis Activity ATTN: AMSXY APG MD 21005-5071
1	Army Dugway Proving Ground STEDP MT M Attn: J. Bowers Dugway UT 84022-5000
1	USACE Engineer Research & Development Center Cold Regions Research and Engineering Laboratory Attn: Dr. Koenig 72 Lyme Road, Hanover, New Hampshire, USA 03755-1290
1	Director, USA TRADOC Analysis Center Attn: ATRC-W (P. Blechinger) WSMR, NM 88002-5502
1	Director, USA TRADOC Analysis Center Attn: ATRC-WA (L. Southard) WSMR, NM 88002-5502

No. Copies	Organization
1	Director, USA TRADOC Analysis Center Attn: ATRC-WEA (D. Mackey) WSMR, NM 88002-5502
1	Director, USA TRAC Anal Ctr Attn: ATRC-FM (T. Bailey) 255 Sedgwick Ave Ft Leavenworth, KS 66027-2345
1	Director, USA TRAC Anal Ctr Attn: ATRC-FMA (T. Gach) 255 Sedgwick Ave Fort Leavenworth KS 66027-2345
1	Director, USA TRAC Anal Ctr Attn: ATRC-FMA (S. Glasgow) 255 Sedgwick Ave Ft Leavenworth, KS 66027-2345
1	United States Military Academy Attn: Combat Simulation Laboratory (Dr. P. West) West Point, NY 10996
1	Battle Command Simulation and Experimentation Directorate Army Model and Simulation Division Attn: DA G37 (DAMO-SBM) 400 Army Pentagon Washington, DC 20310-0450
1	USA PEO STRI Attn: J. Blake 12350 Research Pkwy Orlando, FL 32826-3276
1	HQ USAFA/DFLIB 2354 Fairchild Drive, Suite 3A10 USAF Academy, CO 80840-6214
1	HQ AFWA/DNX 106 Peacekeeper Dr STE 2N3 Offutt AFB NE 68113-4039
1	Naval Research Laboratory Attn: Dr. Goroch Marine Meteorology Division, Code 7543 7 Grace Hopper Ave Monterey, CA 93943-5006

No. Copies	Organization
1	U.S. Naval War College Attn: War Gaming Department (Code 33) 686 Cushing Road Newport, Rhode Island 02841-1207
1	Naval Weapons Surface Ctr Attn: CODE G63 Dahlgren VA 22448-5000
1	JWARS Attn: C. Burdick 1555 Wilson Boulevard, Suite 619 Arlington, VA 22209
1	Northrop Grumman Information Technology Attn: Melanie Gouveia 100 Brickstone Square Andover, MA 01810-5000
1	Anteon Corp. Attn: Mike Adams 46 Growing Rd Hudson, NH 03051
1	Northrop Grumman Corporation Attn: R. Smith E-10A BDT SEIT M&S IPT Lead MS B06-222 2000 NASA Blvd Melbourne, Florida 32907
1	AFRL/IFOIL 525 Brooks Rd Rome NY 13441-4505
1	Tech Connect AFRL/XPTC Bldg 16, Rm 107 2275 D Street WPAFB OH 45433-7226
1	WSMR Technical Library Attn: STEWS IM IT WSMR NM 88002
1	Technical Reports Boulder Laboratories Library Attn: MC 5 325 Broadway Boulder, CO 80305

No. Copies	Organization
1	Ruth H. Hooker Research Library 4555 Overlook Ave, SW Washington, DC 20375
1	U.S. Army Research Laboratory Attn: IMNE ALC IMS Mail & Records Mgmt Adelphi, MD 20783-1197
1 (ELEC)	Admnstr Defns Techl Info Ctr Attn: DTIC OCP (V Maddox) 8725 John J Kingman Rd., Ste. 0944 Ft Belvoir, VA 22060-6218
1	U.S. Army Research Laboratory Attn: AMSRD ARL CI OK TL Techl Lib 2800 Powder Mill Rd. Adelphi, MD 20783-1197
1	U.S. Army Research Laboratory Attn: AMSRD ARL CI OK TP Techl Lib APG, MD 21005

Total: 39 (1 Electronic, 38 CDs)

INTENTIONALLY LEFT BLANK.